

# Signatures of alpha clustering in light nuclei from relativistic nuclear collisions

Wojciech Broniowski<sup>1,2,\*</sup> and Enrique Ruiz Arriola<sup>3,†</sup>

<sup>1</sup>*Institute of Physics, Jan Kochanowski University, 25-406 Kielce, Poland*

<sup>2</sup>*H. Niewodniczański Institute of Nuclear Physics PAN, 31-342 Cracow, Poland*

<sup>3</sup>*Departamento de Física Atómica, Molecular y Nuclear and Instituto Carlos I de Física Teórica y Computacional, Universidad de Granada, E-18071 Granada, Spain*

(Dated: ver. 2, 9 February 2013)

We argue that relativistic nuclear collisions may provide experimental evidence of  $\alpha$  clustering in light nuclei. A light  $\alpha$ -clustered nucleus has a large intrinsic deformation. When collided against a heavy nucleus at very high energies, this deformation transforms into the deformation of the fireball in the transverse plane. The subsequent collective evolution of the fireball leads to harmonic flow reflecting the deformation of the initial shape, which can be measured with standard methods of relativistic heavy-ion collisions. We illustrate the feasibility of the idea by modeling the  $^{12}\text{C}-^{208}\text{Pb}$  collisions and point out that very significant quantitative and qualitative differences between the  $\alpha$ -clustered and uniform  $^{12}\text{C}$  nucleus occur in such quantities as the triangular flow, its event-by-event fluctuations, or the correlations of the elliptic and triangular flows. The proposal offers a possibility of studying low-energy nuclear structure phenomena with “snapshots” made with relativistic heavy-ion collisions.

PACS numbers: 21.60.Gx, 25.75.Ld

In this Letter we show that the nuclear collisions in the ultrarelativistic domain may reveal, via harmonic flow, geometric  $\alpha$  clustering structure of light nuclei in their ground state. As a particular example we present a study of in  $^{12}\text{C}$ , where a triangular structure induces a corresponding pattern in the collective flow.

The  $\alpha$  cluster model was proposed even before the discovery of the neutron by Gamow [1] and rests on the compactness, tight binding  $B_\alpha/4 \sim 7\text{MeV}$ , and stability of the  $^4\text{He}$  nucleus [2–4], which fits into the SU(4) Wigner symmetry of the quartet ( $p \uparrow, p \downarrow, n \uparrow, n \downarrow$ ) (see, e.g., [5] for an early review and [6] for a historic account, while many references can be traced from [7–10]). The remaining weak binding per bonding between the  $\alpha$ -particles,  $V_{\alpha\alpha}/\text{bond} \sim 2\text{MeV}$ , accounts for nuclear binding and makes a molecular picture of light nuclei quite natural. This suggests a vivid geometric view of the self-conjugate  $A = 4n$  nuclei classified by point group symmetries [11]. For instance, in  $^9\text{Be}$  the two  $\alpha$  clusters are separated by as much as  $\sim 2\text{fm}$ ,  $^{12}\text{C}$  exhibits a triangular arrangement of the three  $\alpha$ 's  $\sim 3\text{fm}$  apart,  $^{16}\text{O}$  forms a tetrahedron, etc. The condensation of  $\alpha$  clusters was described in [12] for  $^{12}\text{C}$  and  $^{16}\text{O}$ . Clustering of  $^{20}\text{Ne}$  has also recently been described within the density functional theory [13]. Model calculations are verified by comparing to the experimental binding energies, the elastic electromagnetic form factor, and the excitation spectra. Experimental evidence for clustering comes from fragmentation studies, see, e.g., [14].

Our basic observation and the following methodology stems from the fact that the *intrinsic* wave functions of light  $\alpha$ -clustered nuclei are deformed [15], exhibiting spa-

tial correlation between the location of clusters. Imagine we collide a light  $\alpha$ -clustered nucleus against a heavy nucleus at extremely high energies, as in relativistic colliders (RHIC, LHC) or fixed-target experiments (SPS). During the almost instantaneous passage of the light nucleus through the medium, its wave function collapses, revealing the spatial correlation structure. Let us consider  $^{12}\text{C}$  as an example of a triangular  $\alpha$ -cluster arrangement, colliding with  $^{208}\text{Pb}$ . In a typical collision event, the shape of the created *fireball* in the transverse plane reflects the shape of  $^{12}\text{C}$ , washed out to some degree by different orientations of  $^{12}\text{C}$  and statistical fluctuations. Next, this asymmetric fireball evolves. As the setup is very similar to that in relativistic heavy-ion collisions, we expect collective dynamics to properly model the evolution of the compact dense system, which can be achieved with hydrodynamics (for recent reviews see [16, 17] and references therein) or transport [18] approaches. It has been well established in the studies of relativistic heavy-ion collisions (and even in d-Au and p-Pb collisions [19–24]) that collective dynamics leads to an event-by-event transmutation of the initial anisotropies, described in terms of the harmonic transverse-shape coefficients  $\epsilon_n$ , into the harmonic flow coefficients in the transverse momentum distributions of the produced particles,  $v_n$ . Therefore, applying the well-developed methods [25–28] of the harmonic flow analysis successful in relativistic heavy-ion collisions we may indirectly measure, or assess, the spatial deformation of the initial state. In this Letter we argue that the effects of the  $\alpha$  clustering in light nuclei lead to flow effects which are strong enough to be detectable via ultra-relativistic nuclear collisions.

The mentioned eccentricity parameters  $\epsilon_n$  and the angles of the principal axes  $\Phi_n$  for a distribution of points in the transverse plane are defined as  $\epsilon_n e^{in\Phi_n} = \sum_j \rho_j^n e^{in\phi_j} / \sum_j \rho_j^n$ , where  $n$  is the rank,  $j$  labels the

\* Wojciech.Broniowski@ifj.edu.pl

† earriola@ugr.es

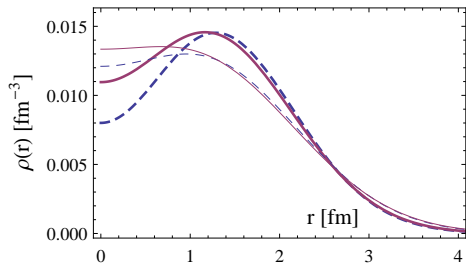


FIG. 1. (Color online) The electric charge density (thin lines) and the corresponding distribution of the centers of nucleons (thick lines) in  $^{12}\text{C}$  for the data and BEC calculations (dashed lines), and for the FMD calculations (solid lines), plotted against the radius.

points, while  $\rho_j$  and  $\phi_j$  are their polar coordinates. The measures  $\epsilon_2$  and  $\epsilon_3$  are referred to as the *ellipticity* and *triangularity*.

We focus our present study on  $^{12}\text{C}$  (the general program is outlined in conclusions), as it leads to interesting properties due to large triangularity. We apply GLISSANDO [29] to carry out the Glauber Monte Carlo ultra-relativistic collisions with  $^{208}\text{Pb}$ . The first task is to properly model the nucleon density of  $^{12}\text{C}$ , including the cluster correlations. The analysis of data for the elastic electromagnetic form factor [30] imposes an important constraint on the charge density [31], which leads to the function indicated with the thin dashed line in Fig. 1 (cf. Fig. 1 of [31]). This distribution is reproduced with the Bose-Einstein condensation (BEC) wave function [32]. On the other hand, calculations based on fermionic molecular dynamics (FMD) [31], which properly reproduce the binding energy, give a somewhat weaker clustering, with the density drawn in Fig. 1 with a thin solid line.

To carry out the NN collisions, we need the distribution of centers of nucleons in  $^{12}\text{C}$ . For that purpose we unfold from the  $^{12}\text{C}$  elastic charge form factor the proton charge form factor, assumed in the Gaussian form  $\text{const} \times \exp(-3/2 r^2/r_p^2)$  with the charge proton radius squared of  $r_p^2 = 0.77 \text{ fm}^2$ . The resulting densities of centers of nucleons are plotted in Fig. 1 with thick lines for the BEC case (dashed) and the FMD case (solid). Note a large central depletion in the distributions, originating from the separation of the  $\alpha$  clusters arranged in the triangular configuration.

Technically, we proceed as follows: The centers of the clusters are placed in an equilateral triangle of side length  $l$ . The nucleons in clusters have a Gaussian radial distribution of the form  $\text{const} \times \exp(-3/2 r^2/r_\alpha^2)$ , from which we randomly generate positions of the 12 nucleons, 4 in each cluster. We take into account the short-distance NN repulsion, precluding the centers of each pair of nucleons to be closer than the expulsion distance of 0.9 fm [33]. Finally, the distribution of 12 nucleons is recentered such that the center of mass is at the origin. The parameters  $l$  and  $r_\alpha$  are optimized such that the thick curves in Fig. 1 are accurately reproduced. This apparently crude

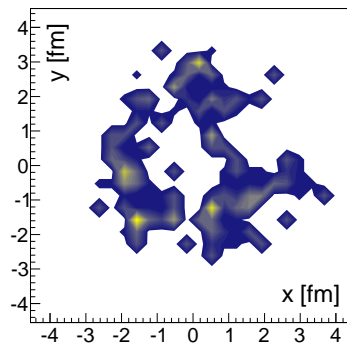


FIG. 2. (Color online) Snapshot of a single central  $^{12}\text{C}-^{208}\text{Pb}$  collision, displaying the distribution of sources in the transverse plane, BEC case,  $N_w = 66$ ,  $N_{\text{bin}} = 93$ . In this simulation the transverse and cluster planes were aligned.

procedure reproduces not only the one-body densities, but also semi-quantitatively ( $\sim 10 - 20\%$ ) the pair densities determined by the multicluster models with state-dependent Jastrow correlations [34]. For the unclustered case we generate the 12 nucleons from a uniform radial distribution of the form  $(a + br^2) \exp(-c^2 r^2)$ , also with short-distance repulsion and recentering. Again, the parameters are adjusted such that the thick lines in Fig. 1 are reproduced.

The resulting two-dimensional projections of the obtained intrinsic distributions are displayed in the left panels of Fig. 3. For the clustered (BEC) case the projection plane is defined by the centers of the three clusters (the *cluster* plane). We note prominent cluster structures for the BEC case (upper left panel). For the uniform distribution (bottom left panel) there is, by construction, no clustering. The results obtained for the FMD case (not presented here for brevity) are qualitatively similar to the BEC case, with somewhat weaker clustering.

We may use the eccentricities to characterize the intrinsic non-spherical nuclear distributions. In the cluster plane the average triangularity for the  $^{12}\text{C}$  distributions equals 0.59 for the BEC and 0.55 for the FMD cases. These are substantial, as the extreme value for point-like clusters is 1. The average triangularity vanishes for the unclustered case. By symmetry, ellipticity is zero. In the plane perpendicular to the cluster plane the average ellipticity equals 0.61 for the BEC, 0.58 for the FMD, and 0 for the unclustered case, while the average triangularity vanishes by symmetry.

Now we are ready to carry out the collisions with  $^{208}\text{Pb}$ , which is prepared in a standard way by uniformly generating 208 nucleons from a Woods-Saxon radial distribution, with the short-distance repulsion taken into account [33]. The Glauber mechanism of the reaction (for a review see, e.g., [35]) proceeds through independent high-energy collisions of the nucleons from  $^{12}\text{C}$  with nucleons from  $^{208}\text{Pb}$ . The concepts of wounded nucleons (those that interacted inelastically at least once) [36] and the binary collisions turn out to be very useful in describing the particle production mechanism. Final multiplicities of the produced particles are properly reproduced if

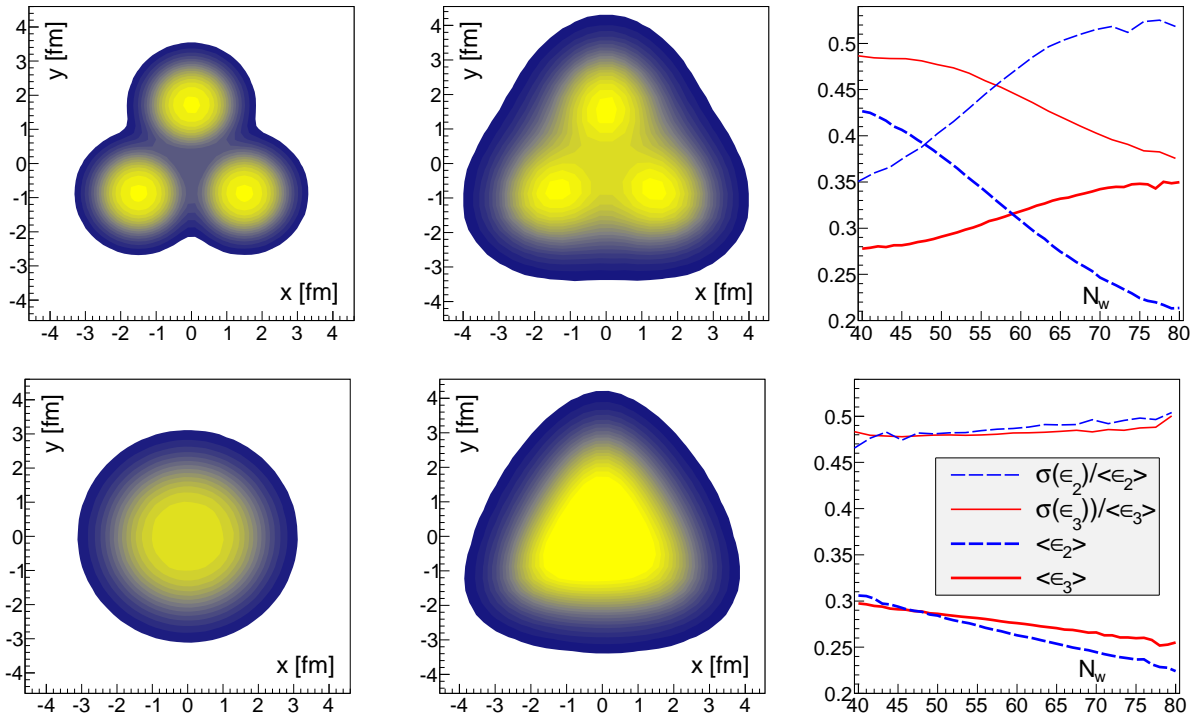


FIG. 3. (Color online) Glauber Monte Carlo simulations with GLISSANDO for the  $^{12}\text{C}-^{208}\text{Pb}$  collisions at the SPS energy  $\sqrt{s_{NN}} = 17$  GeV. The top panels correspond to the clustered BEC case, while the bottom panels display the unclustered case. The left panels show the intrinsic densities in the  $^{12}\text{C}$  nucleus, the middle panels give the corresponding rank  $n = 3$  intrinsic densities of sources in the fireball in the transverse plane for collisions with a high number of wounded nucleons,  $N_w \geq 70$ , and the right panels show the event-by-event statistical properties of the fireball (average ellipticity, triangularity, and their scaled standard deviations) as functions of the number of wounded nucleons. See the text for details.

the initial parton production is proportional to a combination of the number of wounded nucleons,  $N_w$ , and binary collisions,  $N_{\text{bin}}$ , namely  $\sim (1 - a)/2N_w + aN_{\text{bin}}$ , which is the *mixed* model of Ref. [37, 38]. For the collision energies corresponding to the top SPS energy of  $\sqrt{s_{NN}} = 17$  GeV we take  $a = 0.12$ . The total NN inelastic cross section is, at this energy,  $\sigma_{NN}^{\text{inel}} = 32$  mb (all our results do not qualitatively change when  $\sigma_{NN}^{\text{inel}}$  is increased up to the LHC values of  $\sim 70$  mb). We use the realistic Gaussian wounding profile in the simulations [29], meaning that the probability that the two nucleons interact is a Gaussian in their relative impact parameter, of the width controlled by  $\sigma_{NN}^{\text{inel}}$ . The wounded nucleons and binary collisions are jointly referred to as *sources*. The outcome of the Monte Carlo simulation is a distribution of locations of sources in the transverse plane in each event,  $f(\vec{x}) = \sum_j \delta(\vec{x} - \vec{x}_j)$ . In actual applications the sources are *smeared*. This *physical* effect is necessary in preparing the initial condition for hydrodynamics.

A single event of a central (impact parameter equal zero)  $^{12}\text{C}-^{208}\text{Pb}$  collision is shown in Fig. 2. Here we have used the clustered  $^{12}\text{C}$  BEC distribution and aligned the transverse and the cluster planes (the carbon hits the lead “flat”). The shown collision led to 66 wounded nucleons and 93 binary collisions. Note the typical “warped” structure following from the stochastic nature of the process, with the underlying three clusters structure visible.

The eccentricity coefficients of the fireball have two sources. One comes from the average shape (for instance, in non-central A-A collisions the overlap almond-shape region produces  $\epsilon_2$ , or in the present case the triangular cluster shape of  $^{12}\text{C}$  generates triangularity), but, in addition, there is a component from fluctuating positions of the finite number of  $N$  sources. This fluctuating component [39–43] is suppressed with  $N$ . The *intrinsic* density of sources of rank  $n$  is defined as the average over events, where the distributions in each event have aligned principal axes:  $f_n^{\text{intr}}(\vec{x}) = \langle f(R(-\Phi_n)\vec{x}) \rangle$ . Here the brackets indicate averaging over events and  $R(-\Phi_n)$  denotes an inverse rotation by the principal-axis angle in each event. The result of this procedure for generating the intrinsic fireball densities of rank  $n = 3$  is shown in the middle panels of Fig. 3 for high-multiplicity collisions (with more than 70 wounded nucleons). In these simulations the orientation of the  $^{12}\text{C}$  nucleus is in general completely random, however the cut  $N_w > 70$  (imposed for better visibility of the clustering effect) selects preferentially the alignment of the transverse and cluster planes (see the following paragraph). We note the clear traces of the three  $\alpha$  clusters in the middle top panel, while the uniform case (middle bottom panel) is smooth. Note, however, that even the uniform case develops some triangularity, which is entirely due to fluctuations [43].

There is a geometric link between the orientation of

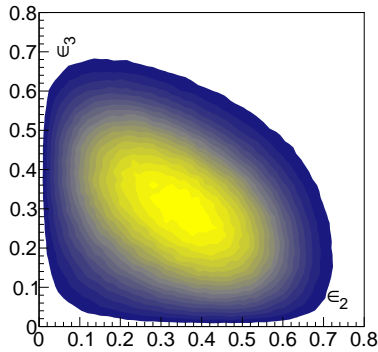


FIG. 4. (Color online) Correlations between ellipticity and triangularity for events with  $N_w \geq 40$  for the BEC clustered case.

the clustered intrinsic distribution of  $^{12}\text{C}$  and the multiplicity of the collision. When the transverse plane and the cluster plane are aligned, the clusters hit the Pb nucleus side-by-side and create most damage, i.e. produce the largest number of sources. In that orientation we have on the average the highest triangularity and the lowest ellipticity (which comes only from fluctuations). On the other hand, when the cluster plane is perpendicular to the transverse plane, we have the opposite behavior: lowest multiplicity, small triangularity, and large ellipticity, which in this case picks up a contribution from the elongated shape of the fireball in the transverse plane. These orientation-multiplicity correlations are crucial for the qualitative understanding of the results in the right panels of Fig. 3.

Quantitative results for the event-by-event averages,  $\langle \epsilon_n \rangle$ , and the scaled standard deviations,  $\sigma(\epsilon_n)/\langle \epsilon_n \rangle$ , for ellipticity and triangularity are shown in the right panels of Fig. 3, where we plot these quantities as functions of the number of the wounded nucleons,  $N_w$ . For the average eccentricities, we can see the advocated behavior from the orientation-multiplicity correlations in the top right panel. We note a significant increase of  $\langle \epsilon_3 \rangle$  with  $N_w$ , and a corresponding decrease of  $\langle \epsilon_2 \rangle$ . For the scaled variances the behavior is opposite, as expected from the division by  $\langle \epsilon_n \rangle$ . For the unclustered case (bottom right panel) the behavior of  $\epsilon_2$  and  $\epsilon_3$  is similar, as both follow from the fluctuations only).

The discussed orientation mechanism also leads to specific correlations of ellipticity and triangularity for the clustered case, as displayed in Fig. 4, where we notice a significant anticorrelation, with the correlation coefficient  $\rho(\epsilon_2, \epsilon_3) \simeq -0.3$ . The unclustered case exhibits no correlations of this kind

The final important point is the relation of the obtained shape parameters of the initial fireball to measurable features in the momentum distributions of produced hadrons. The key result here, following to the *collectivity* of the evolution, is the proportionality of the average values of the harmonic flow coefficients to average ec-

centricities,  $\langle v_n \rangle / \langle \epsilon_n \rangle = A$ , with the constant  $A$  increasing slowly with the particle multiplicity [44–48]. Therefore, for instance, when  $\langle \epsilon_3 \rangle$  increases with multiplicity, so will  $\langle v_3 \rangle$ . For the fluctuation measures the situation a bit more involved due to possibly large contributions to variances at the hadronization stage from the finite number of produced hadrons. Nevertheless, it was found by combining experiment and model simulations that to a good approximation  $\sigma(v_n)/\langle v_n \rangle \simeq \sigma(\epsilon_n)/\langle \epsilon_n \rangle$  [49–51]. It means that in our case the scaled variance of the triangular flow should be significantly larger than for the elliptic flow.

In conclusion, we list the geometric signatures of  $\alpha$  clustering in  $^{12}\text{C}$  to be seen in ultra-relativistic heavy-ion collisions: 1) Increase of  $v_3$  with multiplicity. 2) Decrease of scaled variance of  $v_3$  with multiplicity. 3) Event-by-event anticorrelation of  $v_2$  and  $v_3$ . More sophisticated analysis of the predicted effects should incorporate event-by-event hydrodynamic or transport-model studies, as well as hadronization. Extensions to ultra-relativistic collisions of other light  $\alpha$ -clustered nuclei colliding on heavy nuclei are straightforward and will be presented elsewhere. The reason for the selection of such asymmetric collisions is the fact that in light nuclei the geometric deformation due to  $\alpha$ -clustering is large (the eccentricity parameters are big), while the collision with a heavy nucleus leads to fireballs which are sufficiently large and dense to exhibit well-understood collective behavior in the evolution, leading to harmonic flow. That is not necessarily the case for collisions of two light nuclei.

Hopefully, the possible future data in conjunction with a detailed knowledge of the dynamics of the evolution of the fireball will allow to place constraints on the  $\alpha$ -cluster structure of the colliding nuclei. Conversely, the knowledge of the clustered nuclear wave functions may help to test geometric patterns in fireball evolution models.

From a broader perspective, our proposal may be viewed as an example of study of nuclear deformations/correlations via harmonic flow. For heavy deformed systems (U-U, Cu-Au, as measured at RHIC), certain analyses were recently proposed [52, 53]. For very light-heavy systems the elliptic flow has been detected in d-Au collisions [20], while the proposed studies of the triton-Au or  $^3\text{He}$ -Au collisions at RHIC [21] should look for similar signatures as discussed in this Letter. However, as discussed above, larger systems with intrinsic deformation, such as light nuclei with  $\alpha$  clusters, create larger fireballs whose evolution is expected to be as collective as in the heavy-ion case, thus leading to the eccentricity–harmonic flow transmutation.

This research was supported by the Polish National Science Centre, grants DEC-2011/01/D/ST2/00772 and DEC-2012/06/A/ST2/00390, Spanish DGI (grant FIS2011-24149) and Junta de Andalucía (grant FQM225). WB is grateful to Maciej Rybczyński and ERA to Enrique Buendía for useful conversations.

- 
- [1] G. Gamow, *Constitution of atomic nuclei and radioactivity* (Oxford University Press, 1931)
- [2] J. A. Wheeler, Phys. Rev. **52**, 1083 (1937)
- [3] L. R. Hafstad and E. Teller, Phys. Rev. **54**, 681 (1938)
- [4] W. Wefelmeier, Zeitschrift für Physik **107**, 332 (1937)
- [5] J. Blatt and V. Weisskopf, *Theoretical nuclear physics* (New York: John Wiley and Sons, 1952)
- [6] D. Brink, in *Journal of Physics: Conference Series*, Vol. 111 (IOP Publishing, 2008) p. 012001
- [7] D. Brink, Proc. Int. School Enrico Fermi, Course **36** (1965)
- [8] M. Freer, Reports on Progress in Physics **70**, 2149 (2007)
- [9] K. Ikeda, T. Myo, K. Kato, and H. Toki, *Clusters in Nuclei-Vol.1* (Lecture Notes in Physics **818**, Springer, 2010)
- [10] C. Beck, *Clusters in Nuclei-Vol.2* (Lecture Notes in Physics **848**, Springer, 2012)
- [11] D. Brink, H. Friedrich, A. Weiguny, and C. Wong, Physics Letters B **33**, 143 (1970)
- [12] A. Tohsaki, H. Horiuchi, P. Schuck, and G. Ropke, Phys.Rev.Lett. **87**, 192501 (2001)
- [13] J.-P. Ebran, E. Khan, T. Niksic, and D. Vretenar, Nature **487**, 341 (2012)
- [14] P. I. Zarubin, *Clusters in Nuclei-Vol.3* (Springer, 2014)
- [15] E. Buendía, F. Gálvez, J. Praena, and A. Sarsa, J. Phys. **G27**, 2211 (2001)
- [16] U. Heinz and R. Snellings, Ann.Rev.Nucl.Part.Sci. **63**, 123 (2013)
- [17] C. Gale, S. Jeon, and B. Schenke, Int.J.Mod.Phys. **A28**, 1340011 (2013)
- [18] Z.-W. Lin, C. M. Ko, B.-A. Li, B. Zhang, and S. Pal, Phys.Rev. **C72**, 064901 (2005)
- [19] P. Božek, Phys.Rev. **C85**, 014911 (2012)
- [20] A. Adare *et al.* (PHENIX Collaboration), Phys.Rev.Lett. **111**, 212301 (2013)
- [21] A. M. Sickles (PHENIX Collaboration)(2013), arXiv:1310.4388 [nucl-ex]
- [22] P. Božek, W. Broniowski, and G. Torrieri, Phys.Rev.Lett. **111**, 172303 (2013)
- [23] A. Bzdak, B. Schenke, P. Tribedy, and R. Venugopalan, Phys. Rev. **C87**, 064906 (2013)
- [24] G.-Y. Qin and B. Mueller(2013), arXiv:1306.3439 [nucl-th]
- [25] J.-Y. Ollitrault, Phys. Rev. **D46**, 229 (1992)
- [26] N. Borghini, P. M. Dinh, and J.-Y. Ollitrault, Phys.Rev. **C64**, 054901 (2001)
- [27] S. Voloshin, Nucl.Phys. **A715**, 379 (2003)
- [28] S. A. Voloshin, A. M. Poskanzer, and R. Snellings, in *Landolt-Boernstein, Relativistic Heavy Ion Physics, vol. 1/23* (Springer-Verlag, 2010) p. 5
- [29] W. Broniowski, M. Rybczyński, and P. Božek, Comput. Phys. Commun. **180**, 69 (2009)M. Rybczyński, G. Stefanek, W. Broniowski, and P. Božek(2013), arXiv:1310.5475 [nucl-th]
- [30] H. De Vries, C. De Jager, and C. De Vries, Atom.Data Nucl.Data Tabl. **36**, 495 (1987)
- [31] M. Chernykh, H. Feldmeier, T. Neff, P. von Neumann-Cosel, and A. Richter, Phys.Rev.Lett. **98**, 032501 (2007)
- [32] Y. Funaki, A. Tohsaki, H. Horiuchi, P. Schuck, and G. Ropke, Eur.Phys.J. **A28**, 259 (2006)
- [33] W. Broniowski and M. Rybczyński, Phys. Rev. **C81**, 064909 (2010)
- [34] E. Buendia, F. Galvez, and A. Sarsa, Phys.Rev. **C70**, 054315 (2004)
- [35] W. Florkowski, *Phenomenology of Ultra-Relativistic Heavy-Ion Collisions* (World Scientific Publishing Company, Singapore, 2010)
- [36] A. Bialas, M. Bleszyński, and W. Czyż, Nucl. Phys. **B111**, 461 (1976)
- [37] D. Kharzeev and M. Nardi, Phys. Lett. **B507**, 121 (2001)
- [38] B. B. Back *et al.* (PHOBOS), Phys. Rev. **C65**, 031901 (2002)
- [39] M. Miller and R. Snellings(2003), arXiv:nucl-ex/0312008 [nucl-ex]
- [40] S. Manly *et al.* (PHOBOS Collaboration), Nucl.Phys. **A774**, 523 (2006)
- [41] S. A. Voloshin(2006), arXiv:nucl-th/0606022 [nucl-th]
- [42] W. Broniowski, P. Božek, and M. Rybczyński, Phys. Rev. **C76**, 054905 (2007)
- [43] B. Alver and G. Roland, Phys.Rev. **C81**, 054905 (2010)
- [44] B. Alver *et al.* (PHOBOS Collaboration), Phys.Rev.Lett. **98**, 242302 (2007)
- [45] B. Abelev *et al.* (STAR Collaboration), Phys.Rev. **C77**, 054901 (2008)
- [46] D. Teaney and L. Yan, Phys.Rev. **C83**, 064904 (2011)
- [47] K. Aamodt *et al.* (ALICE Collaboration), Phys.Rev.Lett. **107**, 032301 (2011)
- [48] Z. Qiu and U. W. Heinz, Phys.Rev. **C84**, 024911 (2011)
- [49] B. Alver *et al.* (PHOBOS Collaboration), J.Phys. **G34**, S907 (2007)
- [50] P. Sorensen (STAR Collaboration), J.Phys. **G35**, 104102 (2008)
- [51] G. Aad *et al.* (ATLAS Collaboration), JHEP **1311**, 183 (2013)
- [52] S. A. Voloshin, Phys.Rev.Lett. **105**, 172301 (2010)
- [53] M. Rybczyński, W. Broniowski, and G. Stefanek, Phys.Rev. **C87**, 044908 (2013)